

Next-to-leading Order Photon+Jet Cross Section

Yair Mulian
Institute of Modern Physics

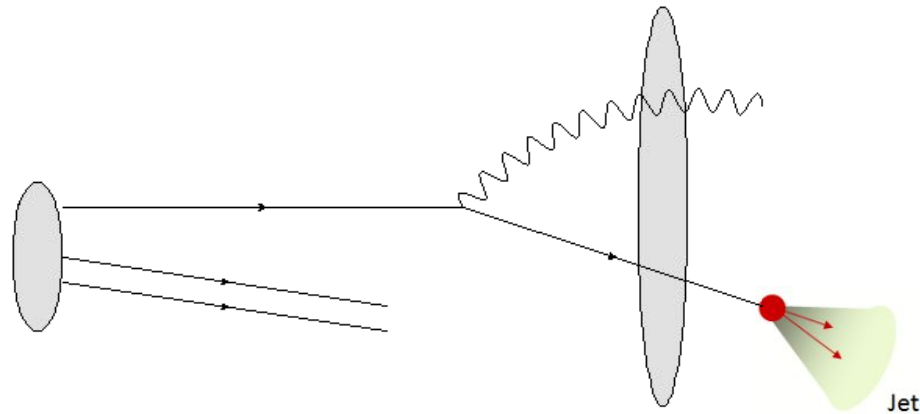
*Light cone 2024,
Huizhou, China*



中国科学院近代物理研究所
Institute of Modern Physics, Chinese Academy of Sciences

Forward jet production

The basic setup: a large- x parton from the proton scatters off the small- x gluon distribution in the target nucleus. The large- x parton is most likely a quark. We adopt the formalism of the LC outgoing state, using the CGC effective theory together with the hybrid factorization.



Quark emitting a photon in the presence of a shockwave.

How to compute the amplitudes?

The time evolution is given by the Schrödinger equation:

$$\frac{d}{dt} |\psi(t)\rangle = -i\hat{H}(t) |\psi(t)\rangle$$

The solution is currently assumed to be given by:

$$|\psi(t)\rangle = \hat{U}(t, t_0) |\psi(t_0)\rangle \quad \hat{U}(t, t_0) = \hat{T} \exp \left[-i \int_{t_0}^t dt' \hat{H}(t') \right]$$

Where $U(t, t_0)$ denotes the evolution operator, known as the Dyson's series,

$$\begin{aligned} \hat{U}(t, t_0) &= \hat{\mathbf{1}} - i \int_{t_0}^t dt' \hat{H}(t') \hat{U}(t', t_0) \\ &= \hat{\mathbf{1}} - i \int_{t_0}^t dt' \hat{H}(t') \left[\hat{\mathbf{1}} - i \int_{t_0}^{t'} dt'' \hat{H}(t'') \hat{U}(t'', t_0) \right] \end{aligned}$$

with H denoting the Hamiltonian of the system.

The state which encodes the information both on the ***time evolution*** and ***interaction with the target nucleus*** is:

$$|\psi\rangle_{out} \equiv \hat{U}(\infty, 0) \hat{S} \hat{U}(0, -\infty) |\psi\rangle_{in}$$

hep-ph/0106240 by
A. Kovner and
U. Wiedemann

The LO outgoing state

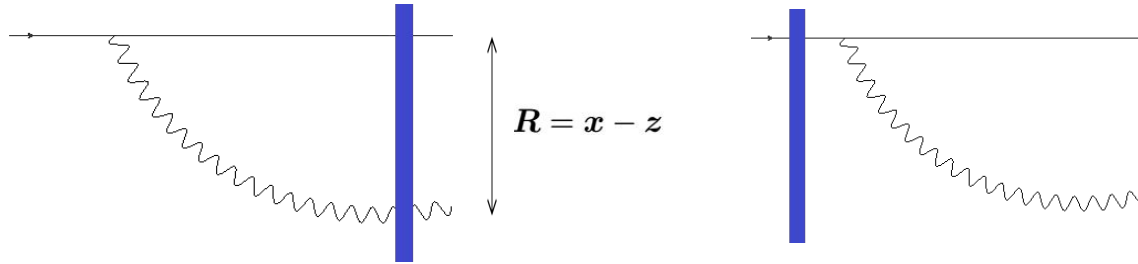
The outgoing state at leading order is given by

$$|q_\lambda^\alpha(q^+, \mathbf{w})\rangle_{out} \equiv U(0, \infty) \hat{S} U(0, -\infty) |q_\lambda^\alpha(q^+, \mathbf{w})\rangle = |q_\lambda^\alpha(q^+, \mathbf{w})\rangle + |q_\lambda^\alpha(q^+, \mathbf{w})\rangle_{q\gamma}$$

The additional term reads:

$$|q_\lambda^\alpha(q^+, \mathbf{w})\rangle_{q\gamma}^{out} = - \int_{\mathbf{x}, \mathbf{y}} \int_0^1 d\vartheta \frac{ig\sqrt{q^+}}{(2\pi)^2} \frac{\phi_{\lambda_1\lambda}^{ij}(\vartheta)}{\sqrt{2\vartheta}} \frac{\mathbf{R}^j}{R^2} \delta^{(2)}(\mathbf{w} - (1-\vartheta)\mathbf{x} - \vartheta\mathbf{y}) \\ \times \left[V^{\beta\alpha}(\mathbf{x}) - V^{\beta\alpha}(\mathbf{w}) \right] |q_{\lambda_1}^\beta((1-\vartheta)q^+, \mathbf{x}) \gamma_i(\vartheta q^+, \mathbf{y})\rangle$$

Diagrammatically:



$$\vartheta \equiv k^+/q^+$$

$$U(x) = \text{T exp} \left\{ ig \int dx^+ T^a A_a^-(x^+, x) \right\}$$

$$V(x) = \text{T exp} \left\{ ig \int dx^+ t^a A_a^-(x^+, x) \right\}$$

Blue bar denotes a shockwave = interaction with the target.

The LO photon+jet cross section

From the outgoing state we can pass easily to the cross section:

$$\frac{d\sigma_{\text{LO}}^{qA \rightarrow q\gamma+X}}{d^3k d^3p} (2\pi)\delta(k^+ + p^+ - q^+) \equiv \frac{1}{2N_c} \text{out}_{q\gamma} \langle q_\lambda^\alpha(q^+, \mathbf{q}) | \hat{N}_q(p) \hat{N}_\gamma(k) | q_\lambda^\alpha(q^+, \mathbf{q}) \rangle_{q\gamma}^{\text{out}}$$

The following number density operators were introduced:

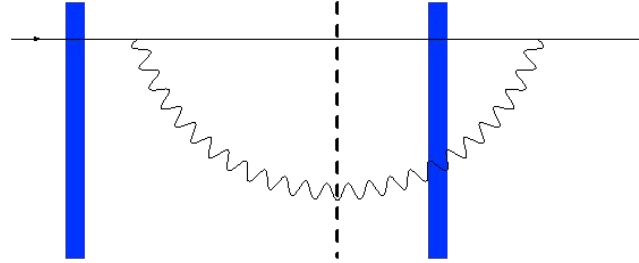
$$\hat{N}_q(p) \equiv \frac{1}{(2\pi)^3} b_\lambda^{\alpha\dagger}(p) b_\lambda^\alpha(p) \quad \hat{N}_g(k) \equiv \frac{1}{(2\pi)^3} a_i^{\dagger}(k) a_i^a(k) \quad \hat{N}_\gamma(k) = \frac{1}{(2\pi)^3} \alpha_i^\dagger(k) \alpha_i(k)$$

The result for the leading-order cross section is given by:

$$\begin{aligned} \frac{d\sigma_{\text{LO}}^{qA \rightarrow q\gamma+X}}{dk^+ d^2\mathbf{k} dp^+ d^2\mathbf{p}} &= \frac{2\alpha_{e.m.}}{(2\pi)^6 q^+} \frac{1 + (1 - \vartheta)^2}{\vartheta} \delta(q^+ - k^+ - p^+) \\ &\times \int_{\mathbf{x}, \bar{\mathbf{x}}, \mathbf{y}, \bar{\mathbf{y}}} \frac{\mathbf{R} \cdot \bar{\mathbf{R}}}{R^2 \bar{R}^2} e^{-i\mathbf{p} \cdot (\mathbf{x} - \bar{\mathbf{x}}) - i\mathbf{k} \cdot (\mathbf{y} - \bar{\mathbf{y}})} \\ &\times [\mathcal{S}(\mathbf{w}, \bar{\mathbf{w}}) - \mathcal{S}(\mathbf{x}, \bar{\mathbf{w}}) - \mathcal{S}(\mathbf{w}, \bar{\mathbf{x}}) + \mathcal{S}(\mathbf{x}, \bar{\mathbf{x}})] \end{aligned}$$

hep-ph/0205037v1 by
F. Gelis and J. J. Marian

An example for contribution which is included in the leading order result:



The dashed line, “the cut”, is the final state (the detector). The dipole is defined by:

$$\mathcal{S}(\bar{\mathbf{w}}, \mathbf{w}) \equiv \frac{1}{N_c} \text{tr} \left[V^\dagger(\bar{\mathbf{w}}) V(\mathbf{w}) \right]$$

From the partonic cross section we can find the quark channel contribution by convolution with the PDF:

$$\left. \frac{d\sigma_{\text{LO}}^{pA \rightarrow q\gamma+X}}{d^3p d^3k} \right|_{q\text{-channel}} = \int dx_p q_f(x_p, \mu^2) \frac{d\sigma_{\text{LO}}^{qA \rightarrow q\gamma+X}}{d^3p d^3k}$$

For measuring a photon+jet one has to convolute the result above with fragmentation/jet function:

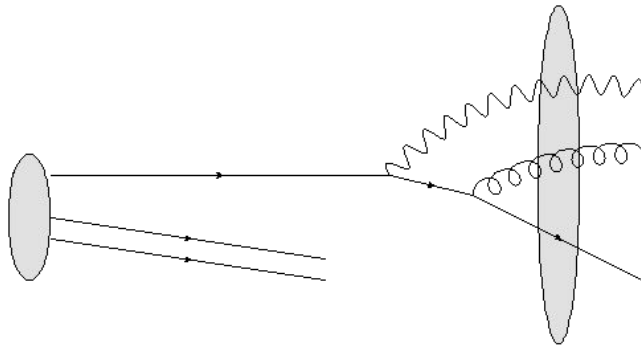
$$\frac{d\sigma_{\text{LO}}^{pA \rightarrow \text{jet}+\gamma+X}}{d^3p d^3k} = \int \frac{dz_1}{z_1^3} \int \frac{dz_2}{z_2^3} \int dx_p q_f(x_p, \mu^2) \frac{d\sigma_{\text{LO}}^{pA \rightarrow q\gamma+X}}{d^3p d^3k} D_{\text{jet}/q}(z_1) J_\gamma(z_2)$$

The dijet+photon setup

Two possible configurations of 3 particles in the final state which are relevant for the cross section at order $\alpha_s \alpha_{e.m.}$

- a) ***Photon, quark and a gluon (quark channel),***
- b) ***Quark, anti-quark and a photon (gluon channel).***

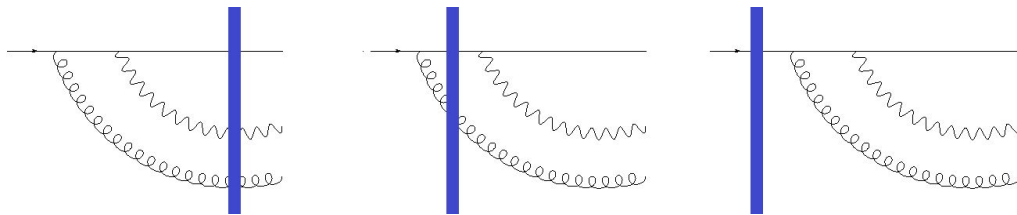
The production of these configurations happen via two successive parton splittings (in the light-cone formalism, there are also 1- \rightarrow 3 instantaneous vertices).



An example for a contribution with 3 particles in the final state

From photon+dijet to “real” NLO photon+jet

Direct and interference (regular and instantaneous emissions):



hep-ph/1810.11273 by T. Altinoluk, R. Boussarie, C. Marquet, P. Taels.

The leading-order contribution to the photon+dijet cross section is:

$$\frac{d\sigma_{\text{LO}}^{qA \rightarrow qg\gamma+X}}{d^3q_1 d^3q_2 d^3q_3} (2\pi)\delta(q_1 + q_2 + q_3 - q^+) \equiv \frac{1}{2N_c} q_{g\gamma} \langle q_\lambda^\alpha(q^+, \mathbf{q}) | \hat{N}_q(q_1) \hat{N}_g(q_2) \hat{N}_\gamma(q_3) | q_\lambda^\alpha(q^+, \mathbf{q}) \rangle_{qg\gamma}$$

The hadronic cross section is given by:

$$\frac{d\sigma^{pA \rightarrow q\gamma g+X}}{d^3q_\gamma d^3q_q d^3q_g} = \int dx_p q_f(x_p, \mu^2) \frac{d\sigma^{qA \rightarrow q\gamma g+X}}{d^3q_\gamma d^3q_q d^3q_g}$$

The real contribution for the NLO photon+jet cross section is related to the partonic cross section by the integration over the unmeasured gluon:

$$\frac{d\sigma_{\text{Rnlo}}^{qA \rightarrow q\gamma+X}}{d^3q_\gamma d^3q_q} = \int d^3q_g \frac{d\sigma^{qA \rightarrow q\gamma g+X}}{d^3q_\gamma d^3q_q d^3q_g}$$

*hep-ph/2009.11930
by Y.M, E. Iancu*

The real cross section

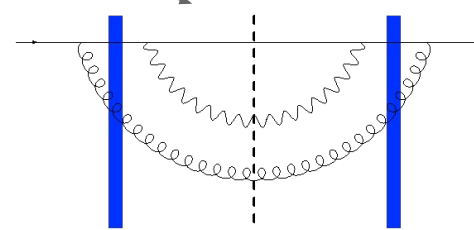
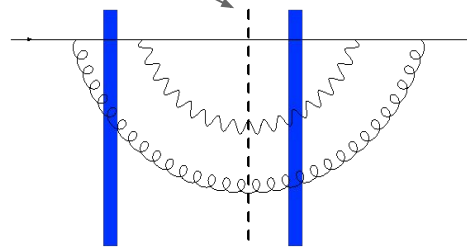
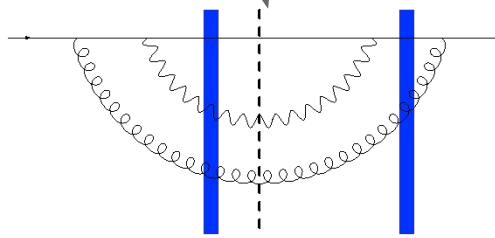
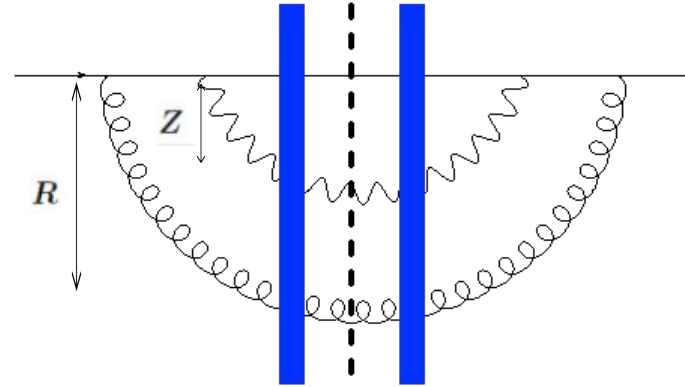
The final combined contribution reads:

$$\frac{d\sigma^{qA \rightarrow q\gamma g X}}{dk_1^+ d^2\mathbf{k}_1 dk_2^+ d^2\mathbf{k}_2 dk_3^+ d^2\mathbf{k}_3} = \frac{\alpha_s \alpha_{e.m.} C_F}{2(2\pi)^{10} (q^+)^2} \delta(q^+ - k_1^+ - k_2^+ - k_3^+)$$

$$\times \int_{\bar{x}, \bar{z}, \bar{z}', x, z, z'} e^{-ik_1 \cdot (x - \bar{x}) - ik_2 \cdot (z - \bar{z}) - ik_3 \cdot (z' - \bar{z}')} \frac{R^i Z^j \bar{R}^m \bar{Z}^n}{Z^2 \bar{Z}^2}$$

$$\times \left[\mathcal{K}_0^{ijmn}(x, z, z', \bar{x}, \bar{z}, \bar{z}', \vartheta, \xi) \mathcal{W}_0(z, z', \bar{z}, \bar{z}') \right]$$

$$\left[-(z, z' \rightarrow y) - (\bar{z}, \bar{z}' \rightarrow \bar{y}) + (z, z' \rightarrow y \ \& \ \bar{z}, \bar{z}' \rightarrow \bar{y}) \right]$$



Similar structure to hep-ph/2009.11930.

The real kernel

The kernel defined by:

$$\begin{aligned} \mathcal{K}_1^{imjn}(x, y, z, \bar{x}, \bar{y}, \bar{z}, \vartheta, \xi, Q) &\equiv \Phi_{\lambda_1 \lambda}^{lirm}(x, y, z, \vartheta, \xi) \Phi_{\lambda_1 \lambda}^{ljrn*}(\bar{x}, \bar{y}, \bar{z}, \vartheta, \xi) \\ &\times \frac{K_1(\bar{Q}D(x, y, z, \vartheta, \xi)) K_1(\bar{Q}D(\bar{x}, \bar{y}, \bar{z}, \vartheta, \xi))}{D(x, y, z, \vartheta, \xi) D(\bar{x}, \bar{y}, \bar{z}, \vartheta, \xi)} \end{aligned}$$

With effective vertex, combining the regular and instantaneous emissions:

$$\Phi_{\lambda_1 \lambda_2}^{ijmn}(x, y, z, \vartheta, \xi) \equiv \varphi_{\lambda_1 \lambda}^{ij}(\vartheta) \tau_{\lambda \lambda_2}^{mn}(\xi, 1 - \vartheta - \xi) - \delta^{nj} \sqrt{\xi(1 - \vartheta)} (\chi_{\lambda_1}^\dagger \sigma^i \sigma^m \chi_{\lambda_2}) \frac{Y^2}{R \cdot Y}$$

And:

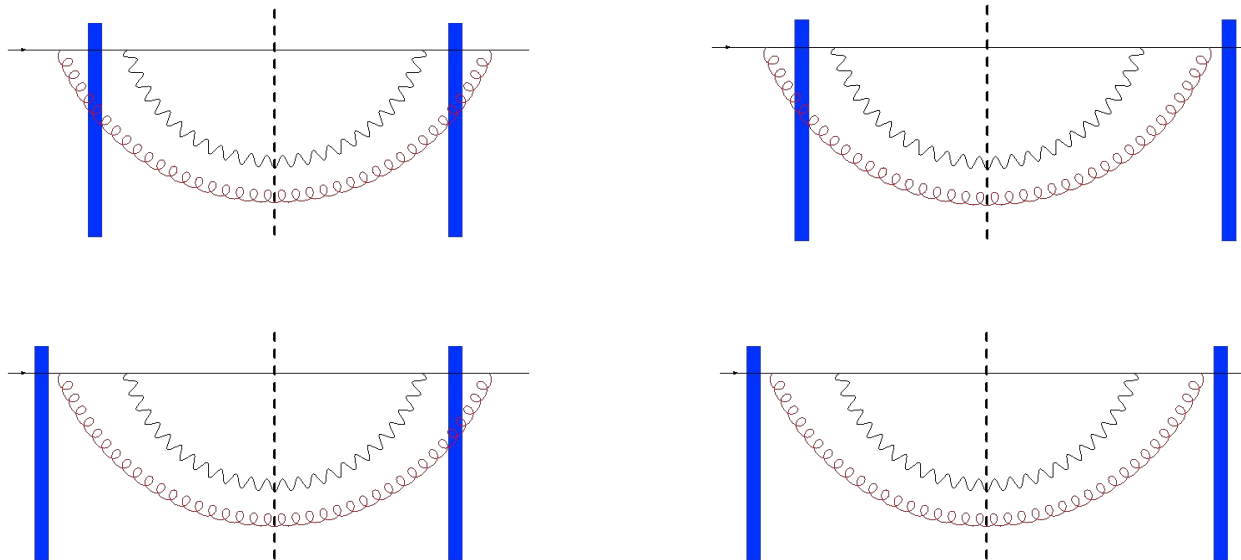
$$\vartheta = \frac{k_1^+}{q^+}, \quad \xi = \frac{k_3^+}{q^+} \quad D(x, y, z, \vartheta, \xi) \equiv \sqrt{R^2 + \frac{\xi(1 - \vartheta - \xi)}{\vartheta(1 - \vartheta)^2} Y^2}$$

Recovering the JIMWLK evolution

In the limit where the gluon become soft (eikonal emission vertex = no recoil of the emitter), the general NLO result has to reduce to one step in the real part of the production JIMWLK evolution of the LO photon+jet production cross section.

$$H = \frac{\alpha_s}{2\pi^2} \int_{\mathbf{x}, \mathbf{y}, \mathbf{z}} \frac{(\mathbf{x} - \mathbf{z}) \cdot (\mathbf{y} - \mathbf{z})}{(\mathbf{x} - \mathbf{z})^2 (\mathbf{y} - \mathbf{z})^2} \left[J_L^a(\mathbf{x}) J_L^a(\mathbf{y}) + J_R^a(\mathbf{x}) J_R^a(\mathbf{y}) - 2J_L^a(\mathbf{x}) U^{ab}(\mathbf{z}) J_R^b(\mathbf{y}) \right]$$

*J. Jalilian-Marian,
E. Iancu,
L. McLerran,
H. Weigert,
A. Leonidov,
A. Kovner/ 97'-99'*

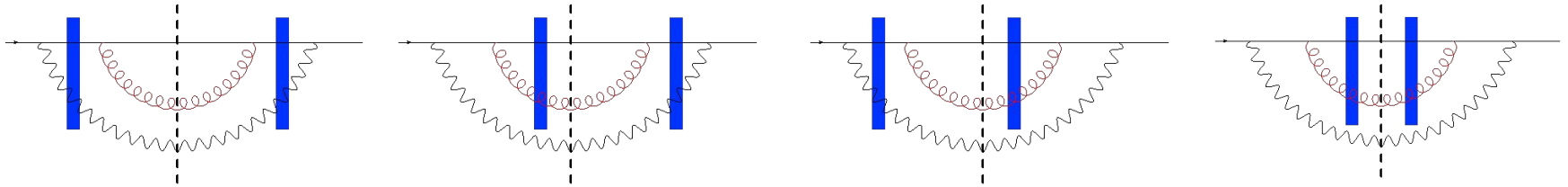


The four diagrams precisely reproduce the the BK evolution of the dipole $\mathcal{S}(w, \bar{w})$ of the leading order cross-section.

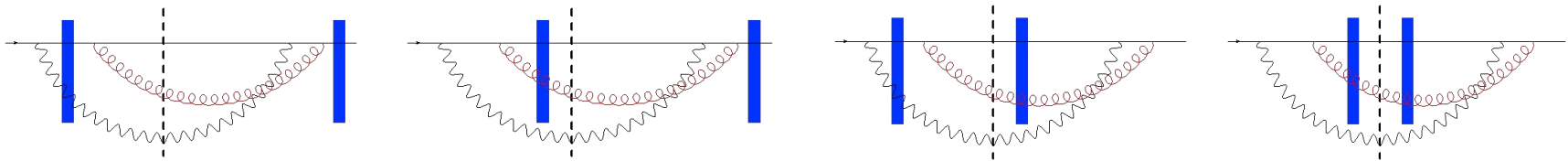
$$\frac{d\sigma_{\text{NLO},1}^{qA \rightarrow q\gamma+X}}{dk_1^+ d^2\mathbf{k}_1 dk_3^+ d^2\mathbf{k}_3} \simeq \frac{\alpha_{e.m.}}{(2\pi)^5} \frac{1 + (1 - \vartheta)^2}{2\vartheta q^+} \delta(q^+ - k_1^+ - k_3^+) \times \int_{\bar{x}, \bar{z}', x, z'} e^{-ik_1 \cdot (x - \bar{x}) - ik_3 \cdot (z' - \bar{z}')} \frac{(x - z') \cdot (\bar{x} - \bar{z}')}{(x - z')^2 (\bar{x} - \bar{z}')^2} \times \frac{\bar{\alpha}_s}{2\pi} \int_0^1 \frac{d\xi}{\xi} \int_z \frac{2(w - z) \cdot (\bar{w} - z)}{(w - z)^2 (\bar{w} - z)^2} [\mathcal{S}(w, \bar{w}) - \mathcal{S}(w, z) \mathcal{S}(z, \bar{w})]$$

→ LO result
→ BK evolution of $\mathcal{S}(w, \bar{w})$

Similarly, the following diagrams generate the evolutions of the dipole $\mathcal{S}(x, \bar{x})$:

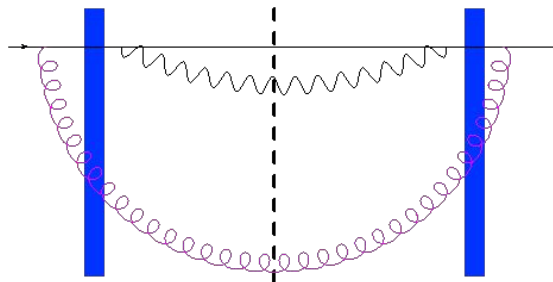
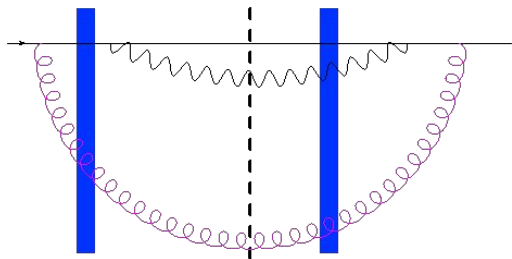
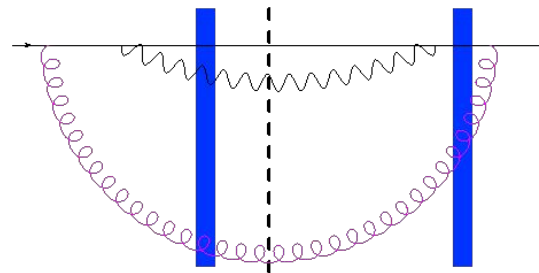
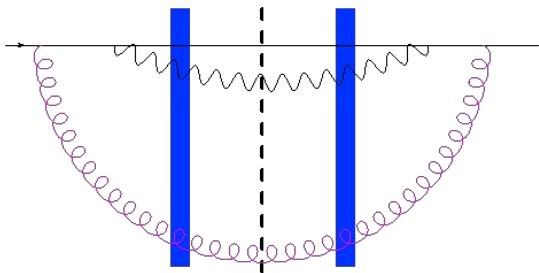


For the dipole $\mathcal{S}(w, \bar{x})$:



Recovering the real DGLAP evolution

In the collinear limit, when the separation between partons become arbitrarily large, we recover the DGLAP evolution of the initial quark pdf and final quark jet function.



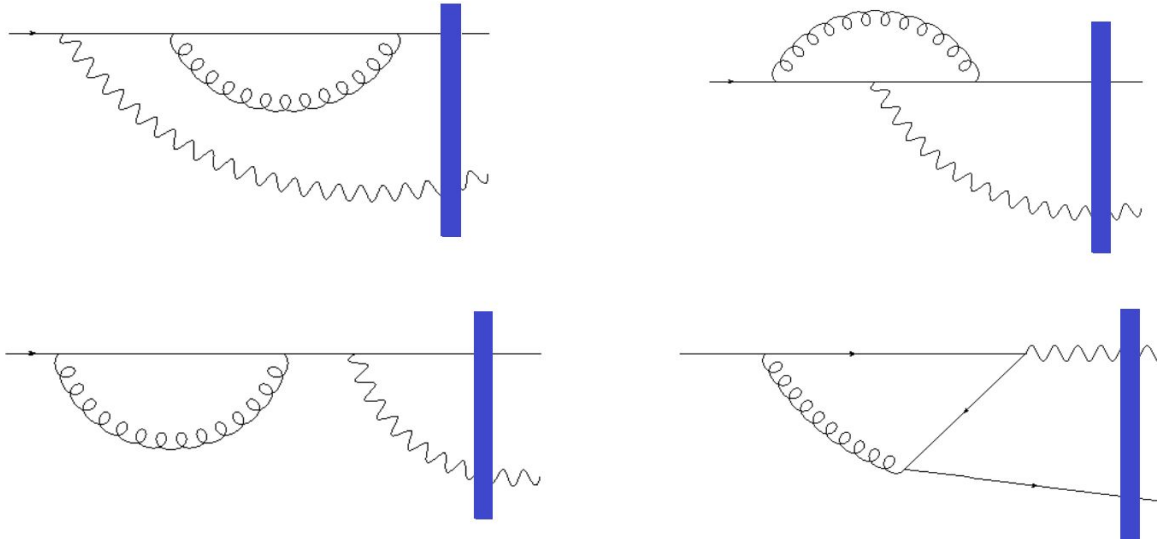
Combining the relevant four contributions:

$$\begin{aligned}
\frac{d\sigma^{qA \rightarrow q\gamma+X}}{dp^+ d^2\mathbf{p} dk^+ d^2\mathbf{k}} &\simeq \frac{4\alpha_{e.m.}}{(2\pi)^6 (q^+)^2 (1-\xi)} P_{q \rightarrow \gamma} \left(\frac{x_2}{x_1 + x_2} \right) \\
&\times \int_{\bar{\mathbf{x}}, \bar{\mathbf{z}}, \mathbf{x}, \mathbf{z}'} e^{-i\mathbf{p} \cdot (\mathbf{x} - \bar{\mathbf{x}}) - i\mathbf{k} \cdot (\mathbf{z}' - \bar{\mathbf{z}}')} \frac{(\mathbf{x} - \mathbf{z}') \cdot (\bar{\mathbf{x}} - \bar{\mathbf{z}}')}{(\mathbf{x} - \mathbf{z}')^2 (\bar{\mathbf{x}} - \bar{\mathbf{z}}')^2} \\
&\times \left[\mathcal{S}(\mathbf{x}, \bar{\mathbf{x}}) - \mathcal{S}(\mathbf{x}, \bar{\mathbf{w}}) - \mathcal{S}(\mathbf{w}, \bar{\mathbf{x}}) + \mathcal{S}(\mathbf{w}, \bar{\mathbf{w}}) \right] \\
&\times \frac{4\alpha_s C_F}{(2\pi)^2} P_{q \rightarrow g}(\xi) \int_{\mathbf{z}} \frac{(\mathbf{y} - \mathbf{z}) \cdot (\bar{\mathbf{y}} - \mathbf{z})}{(\mathbf{y} - \mathbf{z})^2 (\bar{\mathbf{y}} - \mathbf{z})^2}.
\end{aligned}$$

The result above is precisely the result of one “real” step in the DGLAP evolution of the quark distribution inside the proton:

$$x\Delta q_f(x, \mu^2) \equiv \frac{\alpha_s C_F}{\pi} \int_0^{1-x} d\xi \frac{x}{1-\xi} q_f\left(\frac{x}{1-\xi}, \mu^2\right) P_{q \rightarrow g}(\xi) \ln \frac{\mu^2}{\Lambda^2}$$

The virtual contributions



Both UV and IR divergences are involved. Two IR logs appear:

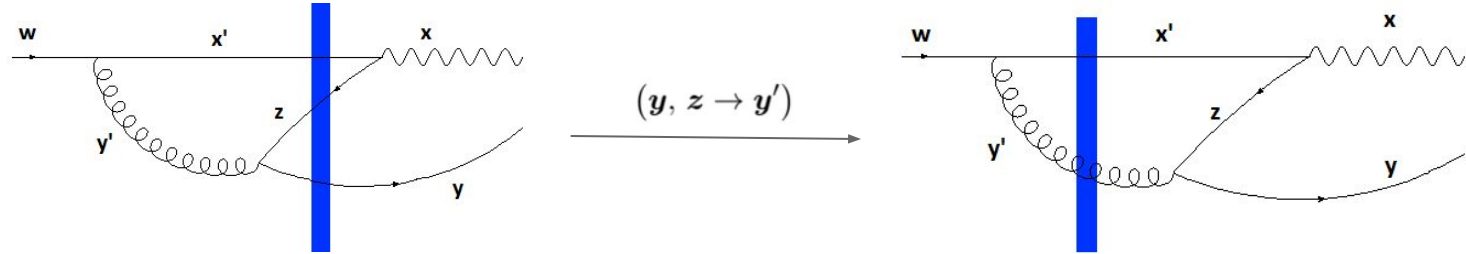
$$\ln\left(\frac{\Lambda}{q^+}\right) \ln\left(\frac{\tilde{k}^2}{\mu_{MS}^2}\right) \quad \ln^2\left(\frac{\Lambda}{\vartheta(1-\vartheta)q^+}\right)$$

hep-ph/2308.02449 by
P. Taels

These are canceled when combining all the various contributions.

Entangled states contributions

Additional class of virtual diagrams involve the shockwave on an intermediate state:



Based on JIMWLK at the S-matrix level, the corresponding cross section was expected to be written in the form:

$$\begin{aligned} \frac{d\sigma^{qA \rightarrow q\gamma+X}}{dk_1^+ d^2\mathbf{k}_1 dk_2^+ d^2\mathbf{k}_2} &= \frac{\alpha_s \alpha_{e.m.} C_F N_f}{2(2\pi)^6 q^+} \delta(q^+ - k_1^+ - k_2^+) \\ &\times \int_{\bar{x}, \bar{y}, x', y, z} e^{-ik_1 \cdot (x - \bar{x}) - ik_2 \cdot (y - \bar{y})} \frac{\tilde{R}^i (X')^j Y^m \bar{R}^n}{\tilde{R}^2 (X')^2 Y^2} \\ &\times \left[\mathbb{K}_0^{ijmn}(x', y, z, \bar{x}, \bar{y}, \vartheta) \mathbb{W}_0(x', y, z, \bar{y}) - \frac{1}{2}(y, z \rightarrow y') \right] \end{aligned}$$

In order to establish this result one has to revise the current formalism and make it compatible with **entangled states**.

Dealing with entangled states



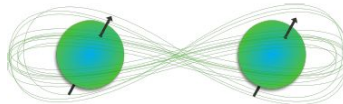
The diagrams above might look similar, but they represent *different* states.

Left: A quark–gluon factorizable state - $|\Psi(k, p)\rangle = |q(p)\rangle |g(k)\rangle$

Right: A quark–gluon entangled (convoluted) state - $|\Phi(k)\rangle = \int dp |q(p)\rangle |g(k - p)\rangle$

Since the Hilbert space for the QCD Hamiltonian is infinite dimensional, the ordering of operations is important. Thus, the norm of these two states has no mathematical justification to be assumed equal to each other:

$$\| |\Psi(k, p)\rangle \| \neq \| |\Phi(k)\rangle \|$$



How to normalize an entangled state?

As long as the state is pure or mixed, the action of \mathbf{N} is equivalent to the rescaling

$$|\psi(t)\rangle \longrightarrow \frac{1}{\mathcal{Z}_\psi} |\psi(t)\rangle$$

With $\mathcal{Z}_\psi \equiv \|\psi(t)\|_{\mathcal{H}}$

For a factorizable quark-gluon state

$$\hat{U}(\infty, 0) |\Psi(k, p)\rangle \rightarrow \frac{1}{\mathcal{Z}_q \mathcal{Z}_g} \hat{U}(\infty, 0) |\Psi(k, p)\rangle$$

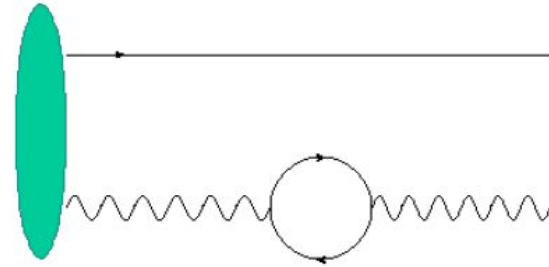
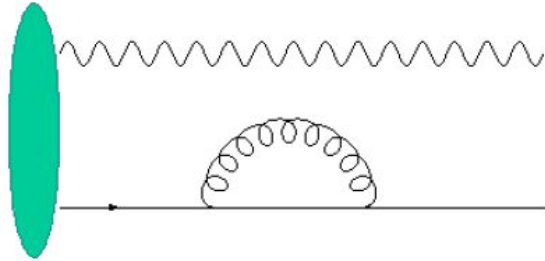
Due to the non-commutativity of integrations on infinitely dimensional spaces,

$$\hat{U}(\infty, 0) |\Phi(k)\rangle \rightarrow \frac{1}{\mathcal{Z}_q \mathcal{Z}_g} \hat{U}(\infty, 0) |\Phi(k)\rangle$$

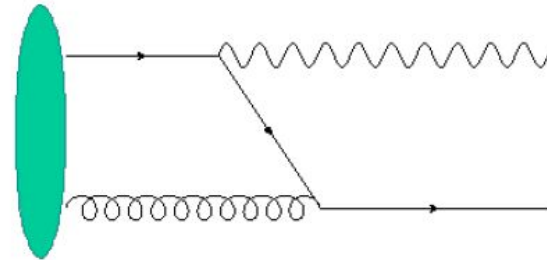
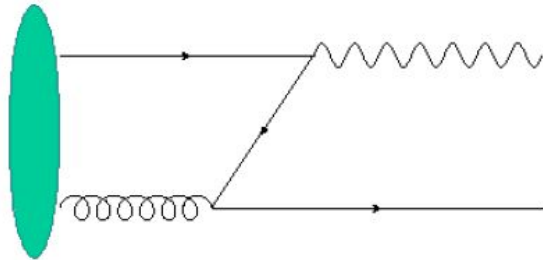
The prescription above can reproduce the self-energy contributions of each participating component but not the exchange contributions. Based on Frobenius:

$$\hat{U}(\infty, 0) |\Phi(k)\rangle \longrightarrow \sqrt{\hat{U}^{\dagger-1}(\infty, 0) \hat{U}^{-1}(\infty, 0)} \hat{U}(\infty, 0) |\Phi(k)\rangle$$

The diagrams generated via the Z factors normalization:



The diagrams which are affected by the operatoric normalization:



The proposal

The solution for the Schrödinger equation is given by a unitarized version of \mathbf{U} :

$$\hat{\mathcal{P}}(t, t_0) \equiv \hat{\mathcal{N}}(t, t_0) \hat{U}(t, t_0)$$

With the new “dynamical normalization operator”:

$$\hat{\mathcal{N}}(t, t_0) \equiv \sqrt{\hat{U}^{\dagger-1}(t, t_0) \hat{U}^{-1}(t, t_0)}$$

See “*On the exact solution for the Schrodinger equation,*”
hep-ph/2402.18499.

Note that unitarity is now **manifest** (no longer based on complex argument):

$$\hat{\mathcal{P}}^\dagger(t, t_0) \hat{\mathcal{P}}(t, t_0) = \hat{U}^\dagger(t, t_0) \hat{U}^{\dagger-1}(t, t_0) \hat{U}^{-1}(t, t_0) \hat{U}(t, t_0) = \hat{\mathbf{1}}$$



Summary

- 1) The results (real and virtual) for the NLO cross section for photon+jet production of an incoming quark are on the way.
- 2) Short-distance poles has been shown to cancel between pairs of diagrams. The IR logs are canceled when combining together the virtual diagrams. Match has been established with JIMWLK (DGLAP) in the eikonal (collinear) limit.
- 3) The Photon+Jet cross section serves as a way to probe the strong force via entanglement that we believe is a promising direction. A new formalism is offered affecting the results for the scattering amplitudes.